

### 3D BIOPRINTING OF VASCULAR CONSTRUCTS

**Kardelen Tüfekçi**

*Molecular Biology and Genetics, 4- Senior*

kardelentufekci@hotmail.com

**Canan Bayraktar**

*Molecular Biology and Genetics, 2- Sophomore*

canan.bayraktar.98@gmail.com

**Melike Çakır**

*Molecular Biology and Genetics, 2- Sophomore*

mell.cakiir@gmail.com

**Miray Turan**

*Industrial Engineering, 1- Freshman*

mirayt@sabanciuniv.edu

**Kemal Ege Kumkumoğlu**

*Computer Science and Engineering, 1- Freshman*

ekumkumoglu@sabanciuniv.edu

**Prof. Dr. Bahattin Koç**

*Industrial Engineering*

#### Abstract

In the additive manufacturing (AM) used for the production of tissues and organs, more commonly known as 3D printing, various types of materials can be used for the bio-ink depending on the type of tissue and different cell types. Several properties of bioink influence the printability including gelation, viscosity, nozzle gauge, shear stress, network properties, and fabrication time. In this project, the construction of vascular structures is aimed by printing of alginate laden cells into a Pluronic® F-127 supporting bath. This work mainly focused on the optimization of the conditions for Pluronic® F-127 for bioprinting. In addition, a model and algorithm to successfully and efficiently print an artery structure with Rhino 3D was developed. Based on optimization studies, it can be said that the storage modulus of the Pluronic® F-127, and the sol-gel transition temperature were found to depend on the concentration of polymer.

**Keywords:** 3D Bioprinting, Pluronic® F-127, Rhino 3D, Bio-ink, Scaffold

## 1 Introduction

The additive manufacturing (AM), more commonly known as 3D printing of biomaterials has a rapid transition from a prototyping research tool into a successful approach for the manufacturing of patient specific medical devices. The key demand is the ability to control structure and material properties in 3D by utilizing the unique anatomical and physiological criteria based on computed tomography (CT) and magnetic resonance imaging (MRI) data (Hinton et al., 2015). Currently, the field is attracting huge attention thanks to the tremendous potential of 3D bioprinting which its main objective is to construct, tissues, organs and other biological systems that mimic their native counterparts (Wobma and Vunjak-Novakovic, 2016).

Depending on the type of tissue and cell types, various types of materials; are needed for the bio-ink and scaffold. The materials used consist of natural and synthetic polymers, living cells, drugs, growth factors and genes. When deposited in a precise and controlled way, it paves the way to the fabrication of not only scaffolds and scaffold-free tissues, but also mini-tissues and organ-on-a chip models. Based on the type of the tissue and goal of the fabrication, different bioprinting methods can be used, including droplet-based, extrusion-based, laser-induced forward transfer, and integrated bioprinting. Each printing technique is based on different physical processes which define the criteria (i.e. rheology profile, photoreactivity, thermal and oxidative stability) of a suitable bio-ink (Donderwinkel et al., 2017). Commonly used materials for bio-inks are hydrogels, which are hydrated networks of crosslinked natural or synthetic polymers. The hydrophilic nature of these polymers allows the gel to swell in an environment with high water content. Hydrogel materials have to be both highly biocompatible and biodegradable, a necessity for in vivo applications. Furthermore, cells can be encapsulated in 3D when the hydrogel undertakes gelation. The created environment does not affect cell survival and cell-cell interactions. The hydrogel suitability for 3D bioprinting depends mainly on its rheological properties and the crosslinking method employed, which can be both physical and chemical in nature. Several properties such as include gelation, viscosity, nozzle gauge, shear stress, network properties, and fabrication time influence printability (Donderwinkel et al., 2017). Hydrogels in tissue engineering must satisfy number specifications to mimic the extracellular matrix (ECM) and as a result they have to perform appropriately to develop new tissue structure. The key functions can be summarized as: (a) encourage cell-biomaterial interactions, (b) promote cell adhesion, (c) permit adequate transport of gases, nutrients and growth factors to ensure cell survival, proliferation, and differentiation, (d) control the structure and function of the engineered tissue (e) deliver the seeded cells to the desired site in the patient's body, (f) confer a negligible inflammation extent or toxicity in vivo, and. (El-Sherbiny and Yacoub, 2013).

Among the bio-printing approaches, extrusion-based printing is mostly used for printing of biological structures. In order to properly construct the structures, bio-inks should have certain viscoelastic characteristics, including shear-thinning and self healing properties in extrusion-based printing. Shear-thinning is important for the extrusion of the bio-ink at low nozzle pressures to protect the cells against physical stressors. The bio-ink should then be able to self-heal to keep an integer 3D printed structure. For a structurally stable complex with mechanical integrity, the bio-ink should harden, in a cytocompatible manner, immediately after printing. Among the natural polymers, alginate, naturally occurring anionic polymer typically obtained from brown seaweed, has been extensively investigated and used for many biomedical applications, due to its biocompatibility, low toxicity, relatively low cost, and mild gelation by addition of divalent cations such as  $\text{Ca}^{+2}$ .

Alginate hydrogels can also be prepared by various cross-linking methods, and their structural similarity to extracellular matrices of living tissues allows wide applications in wound healing, delivery of bioactive agents such as small chemical drugs and proteins, and cell transplantation (Lee and Mooney, 2012). Gelatin is also a natural protein derived from the hydrolysis of collagen, is highly biocompatible and biodegradable in a physiological environment. The presence of aminoacidic sequences such as Arg-Gly-Asp (RGD) in the structure improves the final biological performance of gelatin over synthetic polymers that lack these cell-recognition motifs (Santoro et al., 2014). Pluronics are ABA triblock copolymers consisting of hydrophilic PEG as the A block and hydrophobic polypropylene glycol (PPG) as the B block. Pluronic is a trademark poloxamer with many types that are mostly named with a letter followed by two or three digits. Depending on the Pluronic used, concentration and temperature should be varied. Pluronic F127 (poloxamer 407) is a thermo-responsive hydrogel which has been used as a mould, track patterning and sacrificial material for bioprinting and tissue engineering. It is considered one of the best printable hydrogels due to the nature of micellar-packing gelation, which allows it to be moved and shifted easily. Moreover, the range of its sol-gel transition temperature is broad (10–40 °C), meaning that the viscosity of Pluronic is stable at both room temperature and human body temperature (Suntornnond et al., 2017).

This work mainly focuses on the selection of appropriate hydrogel for 3D bioprinting of vascular constructs, optimization of selected hydrogel's concentration and rheological analysis. In addition to create a model and algorithm to successfully and efficiently print an artery structure.

## **2 Appropriate Conditions for 3D Bioprinting of Vascular Constructs**

### **2.1. Materials and methods**

#### **2.1.1. Selection of hydrogel for supporting bath**

Two different hydrogels were investigated. One of them is gelatin. Gelatin is liquid in room temperature and gel in the cold temperature. If gelatin will be selected, printing must be done in cold. Because of this situation, using gelatin would be harder for printing conditions. Thus, second hydrogel which is called Pluronic® F-127, was examined. Pluronic® F-127 is liquid in cold temperature and gel in the room temperature. If this hydrogel will be used, printing can be made in room temperature. As a result, Pluronic® F-127 was selected and different concentration of this gel was tried.

#### **2.1.2. Preparation and testing of different concentrations of Pluronic® F-127 hydrogels**

2% alginate was prepared by dissolving 1 g alginate in 50 ml PBS. After that, alginate was diluted with 12 ml PBS. 100-200 µl food coloring was added in 1,7% alginate.

Since Pluronic® F-127 was used as supporting bath where the cell laden alginate will be polymerized into a designed structure, Pluronic® F-127 was prepared by dissolving in 1% CaCl<sub>2</sub> solution at 4°C cold room under continuous stirring for 48h. 1% CaCl<sub>2</sub> was prepared by dissolving 2 g CaCl<sub>2</sub> in 200 ml water. Pluronic® F-127 was prepared at different concentrations (16%, 18%, 20%, 25%, 40%) as demonstrated in Table 1.

Concentration of Pluronic® F-127 (%)	Volume of 1% CaCl <sub>2</sub> (ml)	Amount of Pluronic® F-127 (g)
16	50	8
18	50	9
20	50	10
25	50	12,5
40	50	20

**Table 1.** Materials and ratios for preparing Pluronic® F-127.

Concentrations of Pluronic® F-127 at table 1 was tested manually (Figure 1) by using needle.



**Figure 1.** System for testing concentrations manually.



**Figure 2.** System for testing concentrations with printer.

### 2.1.3. Rheology experiment of 16% and 25% concentrations of Pluronic® F-127

The rheometer was set up 4°C and the prepared alginate solutions were placed for the measurement. The programme was set to wait 5 minutes at 4 °C and then the temperature was increased as 5 degrees per minute until 37 °C. Then, gel was waited 30 minutes at 37 °C (Figure 3).

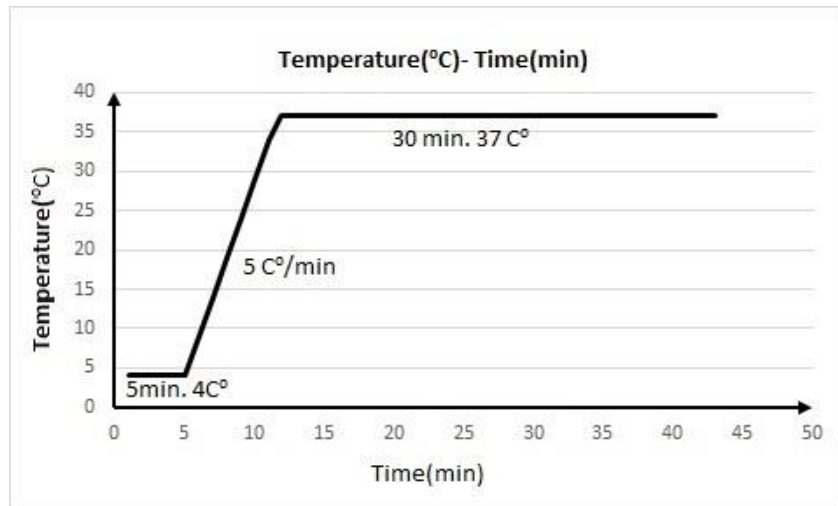


**Figure 3.** Conditions of rheology experiment.

Shear stress and shear rate values would be fit within the model equation by using a regression method (Figure 4).

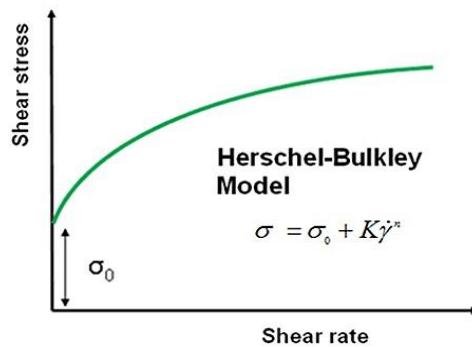


**Figure 4.** Herschel-Bulkley Model.

#### 2.1.4. Create a model and algorithm

We used a program called Rhino 3D to sculpt and model structures that can be used as placeholders for artery structures (Figure 5). After the modeling we moved on to a built-in coding system called Rhino Script that allowed us to take 3D models as inputs and transit them to the 3D printer for the required process. To achieve this we started to design an algorithm to effectively build a bridge between Rhino 3D and the 3D printer. We started with a structure that checks X/Y plane to find intersections. While designing this we assumed the shape of the artery to be cylinder and detected certain intersection points that we named as inner and outer circles. For the inner circles we designated an intersecting point count of 3 and saved the second point to a vector that will later be used as an easy access point for our coordinates. For the upper circle we counted a single intersection because it should be at the very top/ below of our structure. Then we took the saved data and compared them within each other to determine the upper and lower ends of the inner/outer circles. Using these recorded points we determine the WIDTH, RADIUS and CENTER of the 3d structure. In the last and recurring step we determine the inputs we get from the user and the implication of this data. First prominent issue is using the 3D model as in input since the program does not use the same data type as the program. Luckily we were able to find a built in converter to solve that issue. Next was the incorporation of the 3D printer attributes, such as the radius of syringe and rate of printing. Both are taken as variables. The radius of the syringe is used alongside the width, we divide it in a way such that it prints in spirals and starts/ stops  $R/2$  units away from the designed coordinates. The rate of printing is implemented every time the algorithm advances a layer in Z coordinate. The last input we need is the layer width so that we can move the cursor above that much further. Aside from those, the code suffers from over usage of memory and takes a long time to process. As we are trying to make the algorithm work properly and effectively, we are also trying to find ways to make the process smoother and less demanding on the hardware we are using.

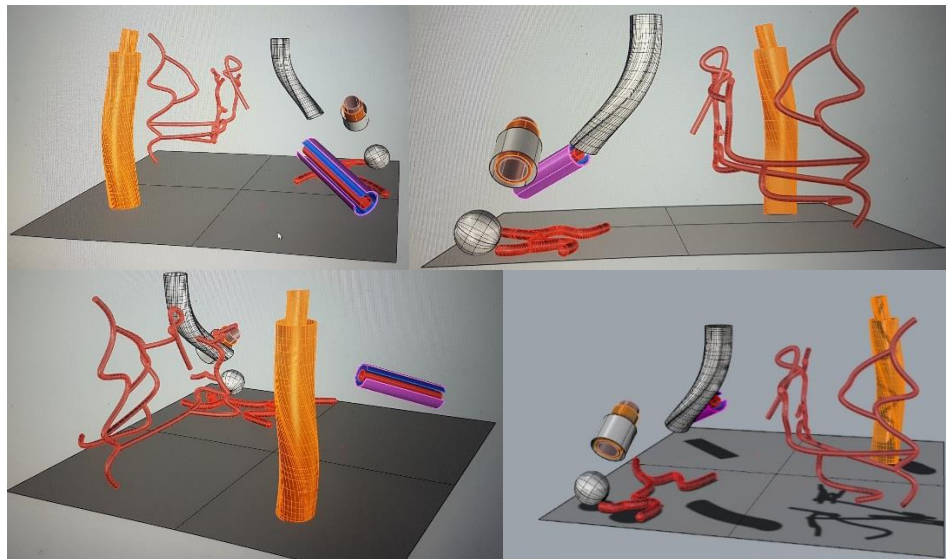


**Figure 5.** Views of artery structure models.

## 2.2. Results

The 16% concentration of Pluronic F127 for supporting bath was too low. Alginate was polymerized due to the presence of  $\text{CaCl}_2$  in the supporting bath, but the supporting bath did not hold the polymerized alginate and it moved with the nozzle (Figure 6). Likewise, gelation time of 16% concentration was too long at  $37^\circ\text{C}$ . The results indicated that 16% Pluronic F127 support bath is not effective to construct desired structure.



**Figure 6.** Testing the suitability of 16% Pluronic F127 supporting bath for bioprinting of alginate.

The concentration of 18% was better than 16% as fiber formation, but gelation time was not enough (Figure 7). Thus, supporting bath did not hold the polymerized alginate.



**Figure 7.** Testing the suitability of 18% Pluronic F127 supporting bath for bioprinting of alginate.

Pluronic F127 with 20%, 25% and 40% were so concentrated that the gel was broken and did not recover itself (Figure 8). Thus, alginate diffused through the rupture before polymerization and fiber formation could not be seen.

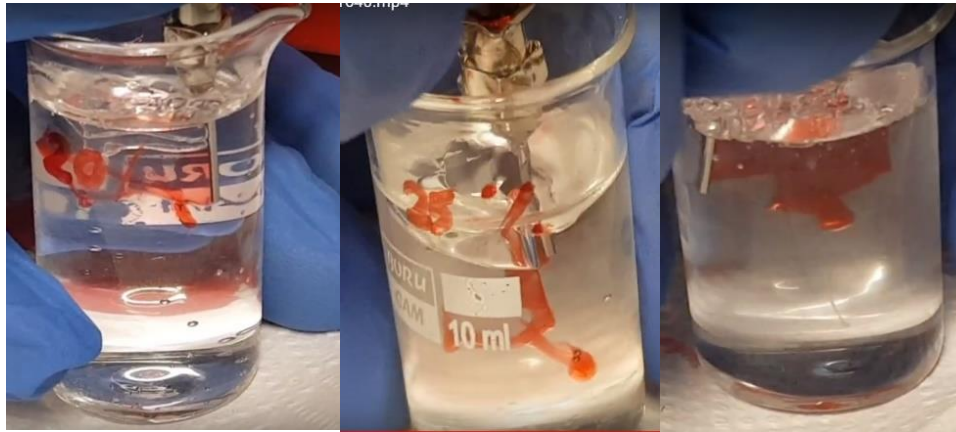


**Figure 8.** Testing the suitability of 20%, 25% and 40% Pluronic F127 supporting bath for bioprinting of alginate.

We also tested the suitability of 22% and 21% concentrations of Pluronic F127. The concentrations of 22% and 21% were prepared by mixing 20% and 25% solutions in an aspected ratio. Briefly, for the 22% solution, 4 ml of 25% solution and 6 ml of 20% solution were mixed. Similarly, 2 ml of 25% solution and 8 ml of 20% solution were mixed to obtain 21% solution. When 22% and 21% Pluronic F127 were tested for the suitability of bioprinting, both concentrations of gels were also broken (Figure 9). We tried the effect of nozzle speed. However, when nozzle speed was decreased from F355  $\mu\text{l}/\text{min}$  to F255  $\mu\text{l}/\text{min}$ , supporting bath was broken again.



**Figure 9.** Testing the suitability of 21% and 22% Pluronic F127 supporting bath for bioprinting of alginate.

We also tried the efficiency of 16% and 18% Pluronic F127 supporting bath by using printer. In order to avoid Pluronic F127 gels to turn back to liquid form at room temperature, the gels were kept at 37°C during printing. We observed that the concentration of 18% was broken again (Figure 10). Although a rupture was not observed at the supporting bath prepared with 16% concentration, the printed shape was not formed since the supporting bath did not hold the polymerized alginate in a certain structure (Figure 11).

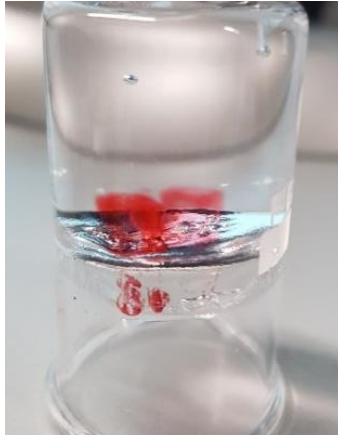


**Figure 10.** The image of polymerized alginate in 18% concentration of Pluronic F127 supporting bath.



**Figure 11.** The image of polymerized alginate in 16% concentration of Pluronic F127 supporting bath.

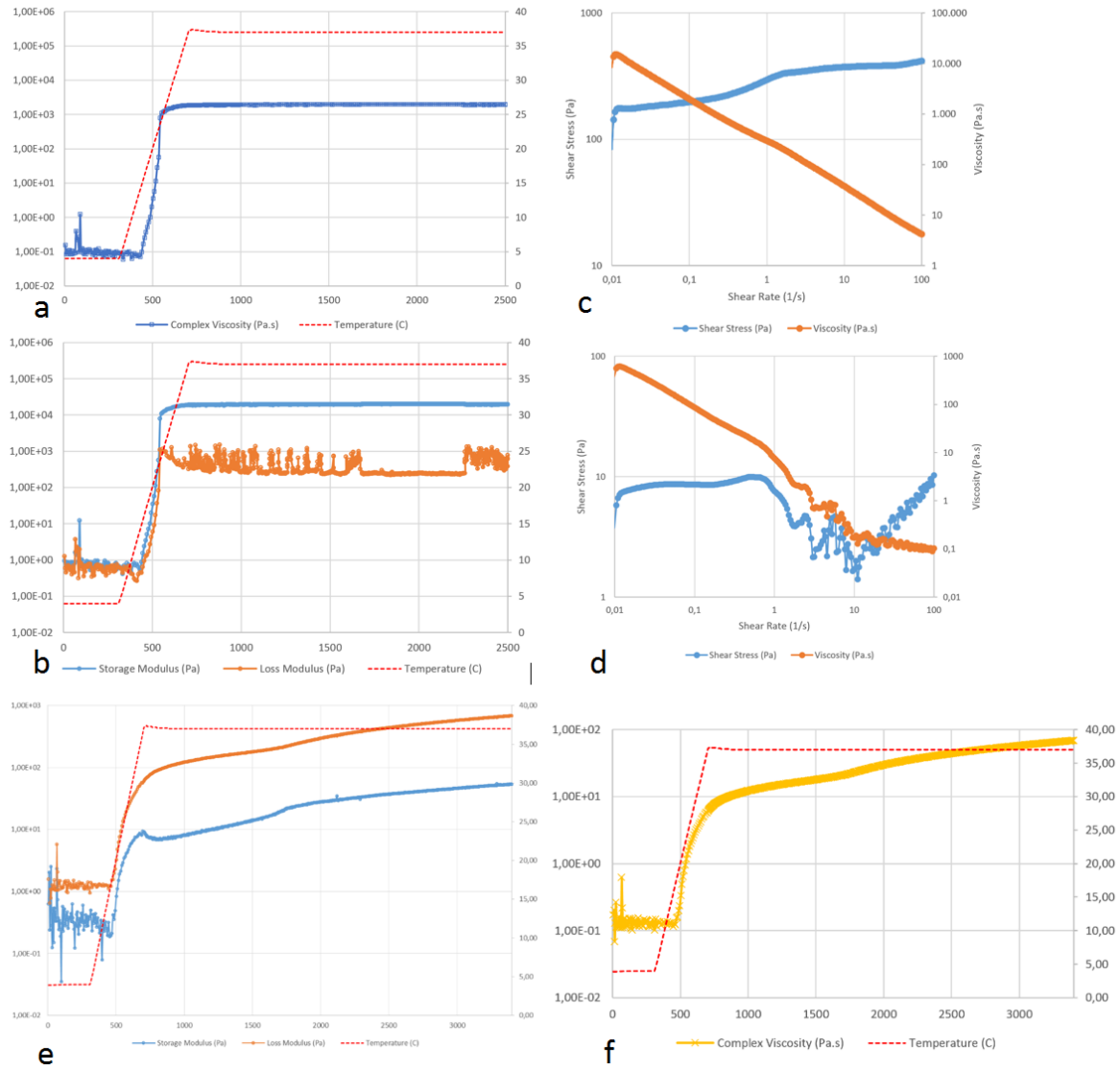


**Figure 12.** Rheological analysis results of 16% and 25% concentrations of Pluronic® F-127. **(a, b)** Viscosity and storage modulus of 25% Pluronic® F-127 as a function of temperature. **(c)** Shear stress and viscosity of 25% Pluronic® F-127 as a function of shear rate. **(e, f)** Viscosity and storage modulus of 16% Pluronic® F-127 as a function of temperature. **(d)** Shear stress and viscosity of 16% Pluronic® F-127 as a function of shear rate.

Gelation at the concentration of 25% was started at room temperature and done at 37 °C. Yield Stress value based on Herschel-Bulkley model was calculated as 163.6 Pa. According to shear stress-shear rate graph, the concentration of 25% causes a linear behavior in the graph and that line breaks under shear stress which indicates that this concentration is not suitable for using.

The gelation at the concentration of 16% was fast and unexpected. Yield Stress value based on Herschel-Bulkley model could not be calculated and it returns the value of -117.4 Pa, which does not make sense in terms of rheology. We can assume that the interactions between the formed micelles are too weak and do not contribute in forming a network showing yield behavior. There is also the possibility that the level of sensitivity of the instrument is not high enough to detect very weak interactions within the formed hydrogel network. According to shear stress-shear rate graph, this concentration is not resistant against needle (Figure 12).

### 3 Conclusion and Future Work

In order to perform 3D tissue engineering, appropriate conditions should be provided, such as optimizing the conditions of the chosen support bath, finding the proper gel concentration and proper environment conditions; as they were tested experimentally whether they are appropriate for tissue engineering or not. It's important that the chosen polymers are bio-compatible where it can provide viability of the encapsulated cells and has cell affinity and reproducible physical and chemical properties. The chosen hydrogel should also be flexible and highly tunable platform for diverse tissue engineering applications, while working with vascular tissues. Gelation time also plays an important role since it is dependent on the concentration of hydrogels.

In this study, alginate was chosen since it can be ionically crosslinked with  $\text{CaCl}_2$  which is an easy process and Pluronic F127 was chosen since it shows thermoreversible polymerization property. Different concentrations of Pluronic F127 were tested to adjust supporting bath conditions. By taking the reference of previously published report, Pluronic F127 (18% w/w; P18) was used (Abrami et al., 2014). Also a graph of "Micellization temperature as a function of the Pluronic F127 concentration" (Jiang et al., 2008) was considered while choosing some of the testing concentrations as well. Primarily, chosen concentrations were tested and observed by external responses such as observing any occurrence of break-through of the gel or fiber structures. Pluronic F127 with 16% and 18% concentrations were tested, as they were waited at room temperature for their gelation formation. The resulted mixture with 16% concentration was not stiff enough to hold the alginate in it as where as 18% showed a stiffer structure while it was in gel form. The subsequent testing concentrations were 20%, 25%, and 40%, as all of them resulted in having tearing of the gel when the alginate was printed in; and the wanted fiber-like structure did not form. Latterly, testing of the Pluronic with 21% and 22% concentrations were decided on, of which results showed that fiber-like structures could not be obtained due to the tearing of the gel during printing. It was decided to keep trying lower concentrations, but by changing other parameters such as temperature. When the mixture for the Pluronic with 16% concentration was kept in a hot bath at 37°C, it seemed to have been reached its gel form as where as it regained fluidic structure when it's kept in room temperature due to its thermoreversible polymerization; which resulted in a decision of printing in Pluronic with concentrations of 16% and 18% while they were kept at 37°C with a heater around them by using the printer other than manually. The results showed that, 16% still was not sufficiently stiff to hold the printed structure while 18% kept having few breakages of the gel when alginate printed, mesh formation and shape fidelity didn't occur but still comparably showed better results.

In the consequence, the rheological properties of Pluronic with 16% and 25% concentrations were tested and observed to see physiological changes. According to shear stress-shear rate graph, the concentration of 25% causes a linear behavior in the graph and that line breaks under shear stress which indicates that this concentration is not suitable for using. We can assume that the interactions between the formed micelles are too weak and do not contribute in forming a network showing yield behavior for 16%. There is also the possibility that the level of sensitivity of the instrument is not high enough to detect very weak interactions within the formed hydrogel network. Based on both previous works and this experiment, it can be said that the storage modulus of the F127 solution, and the sol–gel transition temperature were found to depend on the concentration of polymer (Jiang et al., 2008).

## References

Donderwinkel I., van Hest J. C. M., Cameron N. R. (2017). Bio-inks for 3D bioprinting: recent advances and future prospects. *Polym. Chem.*, 8, 4451–4471. <http://doi.org/10.1039/C7PY00826K>

El-Sherbiny, I. M., & Yacoub, M. H. (2013). Hydrogel scaffolds for tissue engineering: Progress and challenges. *Global Cardiology Science & Practice*, 2013(3), 316–342. <http://doi.org/10.5339/gcsp.2013.38>

Hinton, T. J., Jallerat, Q., Palchesko, R. N., Park, J. H., Grodzicki, M. S., Shue, H.-J., Feinberg, A. W. (2015). Three-dimensional printing of complex biological structures by freeform reversible embedding of suspended hydrogels. *Science Advances*, 1(9), e1500758. <http://doi.org/10.1126/sciadv.1500758>

Jun Jiang, Chunhua Li, Jack Lombardi, Ralph H. Colby, Basil Rigas, Miriam H. Rafailovich, Jonathan C. Sokolov. (2008). The effect of physiologically relevant additives on the rheological properties of concentrated Pluronic copolymer gels. 3561–3567.

Lee, K. Y., & Mooney, D. J. (2012). Alginate: properties and biomedical applications. *Progress in Polymer Science*, 37(1), 106–126. <http://doi.org/10.1016/j.progpolymsci.2011.06.003>

Michela Abrami, Ilenia D’Agostino, Gesmi Milcovich, Simona Fiorentino, Rossella Farra, Fioretta Asaro, Romano Lapasin, Gabriele Grassi and Mario Grassi. (2014). Physical characterization of alginate–Pluronic F127 gel for endoluminal NABDs delivery. *Soft Matter*, 10, 729–737.

Santoro, M., Tataru, A. M., & Mikos, A. G. (2014). Gelatin carriers for drug and cell delivery in tissue engineering. *Journal of Controlled Release: Official Journal of the Controlled Release Society*, 0, 210–218. <http://doi.org/10.1016/j.jconrel.2014.04.014>

Suntornnond, R., Tan, E.Y.S., An, J., Chua, C.K. (2017). A highly printable and biocompatible hydrogel composite for direct printing of soft and perfusable vasculature-like structures. *Sci. Rep.*, 7(1): 16902. <http://doi.org/10.1038/s41598-017-17198-0>

Wobma, H., & Vunjak-Novakovic, G. (2016). Tissue Engineering and Regenerative Medicine 2015: A Year in Review. *Tissue Engineering. Part B, Reviews*, 22(2), 101–113. <http://doi.org/10.1089/ten.teb.2015.0535>